Experimental Determination of Material Boundary Conditions for Computer Simulation of Sheet Metal Deep Drawing Processes

Tomasz Miłek[1*]

[1] Kielce University of Technology, Faculty of Mechatronics and Mechanical Engineering, Al. Tysiąclecia Państwa Polskiego 7, 25-314 Kielce, Poland

* Corresponding author's e-mail: tmatm@tu.kielce.pl

ABSTRACT

In solving technological problems related to sheet metal deep drawing with the use of computer tools, the key issue is still the correct determination and entering of boundary conditions to FEM-based software. The procedure for preparing input data for modelling such processes includes geometric data (drawing of tools and material), technological parameters along with the contact conditions between the workpiece and the tools (friction model and type of lubricant) and material properties, in which work-hardening curves are of particular importance. In typical material databases of FEM-based software and designed for computer modelling of deep drawing processes, the properties of only a small number of material grades are available, and commercial software producers charge additional fees for each additional quantity. Those properties that are already in the database are usually devoid of basic information, e.g. related to the state of the material (material after recrystallization, annealing, cold working has different properties). In paper, experimental tests were carried out to determine flow curves based on cold tensile curves for flat samples made of EN-AW 1050A aluminium, Cu-ETP copper, CuZn37 brass and S235JRG2 steel. The investigation used a universal testing machine with a 20 kN pressing force, equipped with specialized Test&Motion software for measuring forces and displacements. It was calibrated and satisfies the metrological requirements for class 0.5. A comparative analysis of the curves determined by the analytical method was carried out. The material models obtained in the experimental tests were used in the computer simulation of the deep drawing processes of cylindrical drawpieces in the ABAQUS software. The results were experimentally verified in terms of comparing the changes in the pressing forces as a function of the displacement of the punch. The results obtained in the research can be used in industrial practice for computer-aided design of cold-deep drawing processes for drawpieces of various shapes from the discussed materials.

Keywords: FEA, deep drawing, metal forming, computer modelling, flow curves, engineering processes.

INTRODUCTION

Materials intended for deep drawing processes should be characterized by right formability (drawability), corrosion resistance, appropriate mechanical properties and lack of internal defects. Among the material properties that may affect the drawability of the sheet, the most important are: ability to hardening, sensitivity on velocity of deformation, homogeneity of the structure and normal anisotropy [1]. While maintaining a constant values of parameters such as strain rate, temperature, pressure, the flow stress σ_p depends only on the strain φ. This relationship determined experimentally is represented by the strengthening curves [2]. The diagram covers only the initial sections of the strengthening (hardening) curves, but this is the range of deformations occurring in most sheet metal stamping processes. In the literature on the subject [2, 3], various methods of experimental determination of the initial sections of the strengthening curves for sheets are discussed, e.g. such as:

- method of uniaxial stretching of a flat sample with simultaneous recording of the tensile force as a function of the sample's measuring length,

- a method of compressing a package made of many sheet metal blanks,
- a method of shaping material from a blank of sheet metal fixed at the circumference by means of liquid pressure,
- method of determining a three-parameter strengthening curve passing through three given points on the experimental curve.

For materials in the annealed condition (when $\varphi_0 = 0$), the three-parameter hardening curve is usually simplified to a two-parameter form. In this case, much simpler methods are used to determine it, described in literature [2, 3].

In solving technological problems related to sheet metal deep drawing using computerized tools, a key issue is still the correct definition and input of boundary conditions into FEM-based programs. The procedure for preparing input data for modeling such processes includes geometric data (tool and material outline), technological parameters along with tool-material contact conditions (type of lubricant), and material properties, in which the strengthening curves are of particular importance. In typical material databases of FEA-based programs for computer modelling of deep drawing processes, the properties of only a small number of material grades are available, and commercial software developers demand additional fees for each additional quantity. Those properties that are already in the database usually lack basic information, e.g. regarding the state of the material (material in the as-delivered condition, annealed or strengthened state has different properties). In computer programs based on FEM, intended for the simulation of various metal forming processes, the strengthening curve for a specific material can be entered in three ways: by means of an equation (function), by manually entering the points of the curve or by loading a text file from the experiment according to strictly defined recommendations (with properly arranged columns for different temperatures and deformation rates).

As part of the introduction to this work, a review of several dozen recently published papers devoted to the analysis of material hardening, analytical and experimental development of strengthening curves and their use for computer simulation of the process of deep drawing drawpieces of various shapes. The papers also describe issues related to the input of data for modelling as material boundary conditions and some problems arising during the shaping of drawpieces and thin-walled products. The results of some of them [4-18] are discussed below.

Gronostajski Z. with his team of peers composed of scientists from several Polish academic centres [4] presented the latest development trends in the field of metal forming, including deep drawing processes, both from experimental and numerical point of view. The authors highlight that numerical simulations are not only currently used to predict mechanical states including deformations, stresses and forces, but also enable the prediction of microstructure development and the thermo-mechanical-metallurgical approach. The study discusses different aspects associated with computer modelling with the use of original, recently developed solutions of the authors. Rousselier G. et al. [5] developed own approach for modelling of anisotropic hardening and non proportional loading paths in application to numerical analysis of deep drawing of cup made from strongly anisotropic 2090-T3 aluminium-lithium alloy 1.6 mm thick sheet sample. The model of the material presented in the paper, based on the experimental hardening curve, was used to simulate the deep drawing of cups in the ABAQUS software. They compared the computer simulations with the experimental results in terms of the height of the drawpieces, showing a good agreement between the results. In their study, Merklein and Gödel [6] compared the work hardening of material under different test conditions. In numerical simulation of deep drawing process the flow behaviour of the material is described by the hardening curve under uniaxial stress condition. In their opinion in a standard tensile test, experimental values can only be determined up to small deformations, therefore additional experimental tests are needed to obtain larger deformations for the material characteristics. In the paper, they presented the results together with the analysis of two tests under biaxial loading (the bulge test and the layer compression test) and one test under uniaxial stress condition (the tensile test but after the onset of necking by using contraction started, which was assessed using an optical strain measurement system). The tests were carried out for samples with a thickness of 0.7 mm made of DX56 steel. They demonstrated that all tests give the possibility to determine the hardening curve for higher strains and offer the same results, but the bulge test and the layer compression test are more laborious than the evaluation using the optical strain

measurement system ARAMIS. Bressan J et al. [7] conducted comparative studies of numerical and experimental graphs of force changes as a function of displacement for the deep drawing process of drawpieces made from five types of steel sheets (DQSK, BH33, HSLA50, TRIP600 and DP600) and sheet of AA6022 aluminium alloy. However, the authors in the work did not provide the shape and dimensions of the tested drawpiece. Computer modelling was carried out in the AutoForm software. Experimental results and material characteristics in the form of strengthening curves were used from a doctoral thesis from a Technical University of Denmark. The authors in the paper [7] did not provide a method for determining the coefficients in the strengthening curves used in the simulations. Trzepieciński and Gelgele [8] carried out numerical and experimental research of deep drawing process of rectangular drawpiece made from DDQ steel sheet with a wall thickness of 1 mm. For the simulation, 3D model was used in the ABAQUS software. In the material description of the FEM model was implemented a two-parameter strengthening curve and Hill's yield criterion. Parameters of Hollomon's equation were determined in a tensile test. Trzepieciński and Gelgele [8] demonstrated that together with friction anisotropy condition, their model gave simulation results that can better approximate the experimental measurements. In their studies, Peters et al. [9] modified the existing material model in the commercial LS-Dyna software. The changed model takes into account the dependence of its parameters on the equivalent plastic strain and the relationship between the strain rate and the yield stress. The model was successfully verified by means of experimental deep drawing tests for steel and aluminium alloy. The experimental results were used to fit the parameters of the material model. Dizaji et al. [10] demonstrate influence of different hardening models (isotropic, kinematic and combined hardening rules) on the various uncoupled ductile fracture criteria. They implemented the cracking criteria into the ABAQUS finite element code. Authors [10] carried out an experimental verification of the model for the deep drawing of cylindrical drawpieces made from DKP 6112 steel. The parameters of the two-parameter strengthening curve were determined in a uniaxial tensile test without presenting the calculations in paper [10]. El-Aty et al. [11] presented a summary of their research over the last few years on the hard-

ening, anisotropy and deformation of Al-Li alloys. The authors [11] investigated the strengthening mechanisms and formability of these alloys depending on chemical composition, processing and microstructural interactions.

In their studies, Ruiz-Pinilla et al. [12] proposed analytically determined hardening curves for iron-based shape memory alloys (Fe-SMA) using modified Ramberg-Osgood models for nonlinear materials. The authors [12] developed them based on experimentally obtained stress-relative strain diagrams in the tensile test. It was conducted under displacement control in a Z100 Zwick universal testing machine. Hardening curves were implemented into a material finite element model (ATENA software) developed to reproduce the response of reinforced concrete beams strengthened upon shear using external Fe-SMA strips. Feng et al. [13] conducted comparative studies of micro- and macro-mechanical constitutive models for an aluminium alloy. The developed relationships between deformation and stress were used for computer simulations of the deep drawing process of cylindrical drawpieces in the ABAQUS software. Authors [13] used additional alloy experimental data, such as Lankford R coefficients and anisotropic yield surface evolution, to validate implemented the models.

Walzer et al. [14] demonstrate that the local increase in yield strength contributes to preventing premature sheet thinning in the force transmission zones and avoid split formation in early stages of a deep drawing process of drawpieces made from DP600 steel sheets having a thickness of 1.2 mm. In the material model, they used experimentally determined flow curves, which were analytically approximated by using the isotropic plasticity criterion of Ludwik-Hollomon. This model was used to simulate the deep drawing process in the STAMPACK software [14].

In a very extensive study [15], covering the results of tests by eleven research teams, an analysis of the results of deep drawing of a cups with 1 mm thick aluminium sheet was presented. Ready-made commercial or self-developed material models based on various constitutive relationships were used in modelling the process. The characteristics of material was conducted by tensile tests, biaxial tensile tests, monotonic and reverse shear tests and EBSD measurements.

In the available papers on the simulation of deep drawing processes, examples of which are presented above [4-18], the authors in the vast

majority of cases do not present the methodology or calculations involved in the determination of the usually simplified two-parameter equations of the strengthening curves used as material boundary conditions. In fact, this is not peculiar to stamping processes, as a similar problem applies to volume forming processes such as upsetting [16] or radial [17] and backward extrusion of material [18]. In the opinion of the author of this study, there is still a need in industrial practice to have access to experimental results that can be adopted as input data for modelling various metal forming processes. The main aim of the research in the work was to determine experimental strengthening curves for four materials: EN-AW 1050A aluminium, Cu-ETP copper, CuZn37 brass and S235JRG2 steel, and to approximate their three-parameter function so that they could be used as boundary conditions in simulations of cold deep drawing processes of drawpieces with various shapes. A comparative analysis of the curves determined by the analytical method was carried out. The material models obtained in the experimental tests were used in the computer simulation of the deep drawing processes of cylindrical drawpieces in the ABAQUS software. The results were experimentally verified in terms of comparing the changes in the pressing forces as a function of the displacement of the punch. On the basis of obtained results, it is possible to comprehensively evaluate the selected materials and use the data from the Author's work to study the deep drawing processing of cylindrical drawpieces.

METHODOLOGY

The experimental tests described in this paper were carried out on a LabTest 5.20SP1 (LABORTECH) testing machine (shown in Figure 1). It meets the metrology requirements for class 0.5 in the measurement range from 0.2 kN to 20 kN for the relative error values of the force measurement system and the relative resolution of the force indicator. The machine was equipped with specialised Test@Motion software for handling experiments. The software allowed force changes to be recorded as a function of displacement. The strain rate during the tests was 10 mm/min and was the same for all materials.

EN-AW 1050A aluminium, Cu-ETP copper, CuZn37 brass and S235JRG2 steel test pieces were used in investigations. The selected materials is used in industrial sheet metal forming in a wide field of applications especially for parts with complex geometry shapes. The test specimens were not annealed because it is common in industrial practice to use the material for stamping in the as-delivered
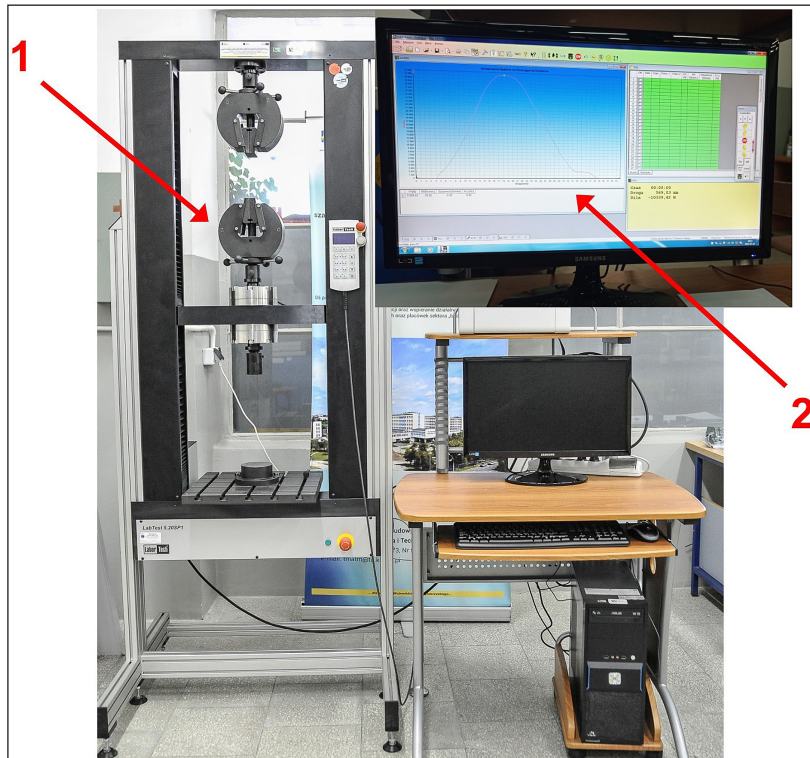

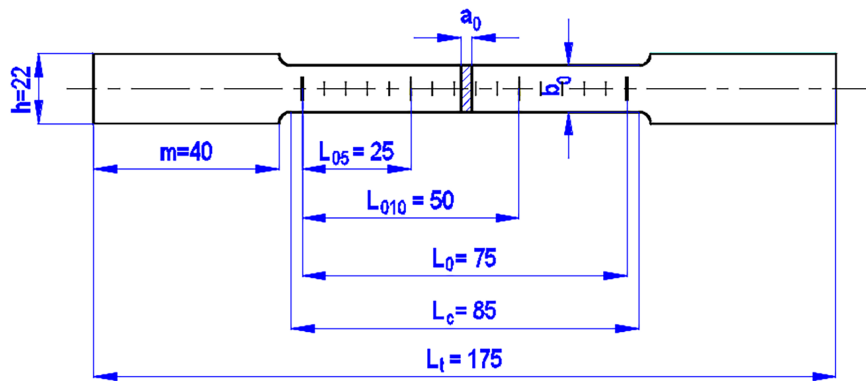**Fig. 1.** View of LabTest 5.20SP1 testing machine (1) with Test@Motion software (2)

Fig. 2. The shape of the test pieces used in the experiment

condition. The mechanical properties of the materials were determined in a static tensile test [19]. The shape and dimensions of the test pieces before deformation are shown in Figure 2. The samples were cut from the sheet in the direction of rolling. Table 1 shows the results of the measurements and the maximum tensile forces for each material. The tensile test graphs obtained are shown in Figure 3. The mechanical properties for aluminium, copper, brass and steel are shown in Table 2. They were obtained based on measurements and calculations according to ISO 6892-1 [19]. The L_{05} and L_{010} measurement bases (as shown in Figure 2) were used to determine the percentage elongations after fracture A and $A_{11.3}$, respectively. The proof strength, plastic extension, $R_{p0.2}$ (yield strength) were determined using a graphical method at a strain of 0.2%. The engineering software *Grapher* was used to determine them.
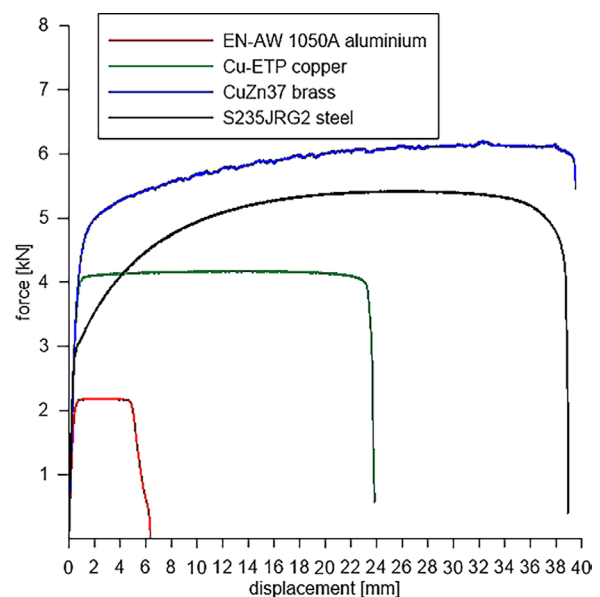

Fig. 3. The force vs. displacement (ΔL) obtained for tensile tests

Table 1. Dimensions of test pieces and values of maximum tensile forces obtained in the tests

Material	b_0 (mm)	a_0 (mm)	L_5 (mm)	L_{10} (mm)	S_0 (mm²)	F_m (N)
EN-AW 1050A aluminium	17.61	1.03	28.90	54.64	18.14	2184
Cu-ETP copper	16.93	0.99	40.90	77.82	16.76	4176
CuZn37 brass	16.79	0.99	38.30	72.60	16.62	6177
S235JRG2 steel	16.93	1.01	41.16	76.40	17.10	5424

Table 2. Mechanical properties of test pieces used in the investigations

Material	R_m (MPa)	$R_{p0.2}$ (MPa)	A (%)	$A_{11.3}$ (%)
EN-AW 1050A aluminium	120.4	111	16	9
Cu-ETP copper	249.2	239	64	56
CuZn37 brass	371.6	289	53	45
S235JRG2 steel	317.2	189	65	53

The experimental strengthening curves determined in the next stage of the research were described using a three-parameter power function (1) passing through three given points that satisfy the system of three equations (2) [2]:

$$\sigma_p = C \cdot (\varphi_0 + \varphi)^n \tag{1}$$

where: σ_p – flow stress, MPa;
  C – constant dependent on the mechanical properties of the material, MPa;
  φ_0 – initial logarithmic strain;
  φ – logarithmic strain;
  n – strengthening curve exponent.

$$\begin{aligned} \sigma_{pA} &= C_1 \cdot (\varphi_0 + \varphi_A)^n \\ \sigma_{pB} &= C_1 \cdot (\varphi_0 + \varphi_B)^n \\ \sigma_{pC} &= C_1 \cdot (\varphi_0 + \varphi_C)^n \end{aligned} \tag{2}$$

The method of determining the points [2] is shown in Figure 4. The solution to the system of equations (2) can be obtained only when the intermediate stress (corresponding to the intermediate point C) is the geometric mean of the two extreme stresses (corresponding to the extreme points A and B):

$$\sigma_{pC} = \sqrt{\sigma_{pA} \cdot \sigma_{pB}} \tag{3}$$

The values of φ_0 and the exponent n were determined from formulas (4) and (5) respectively [2]:

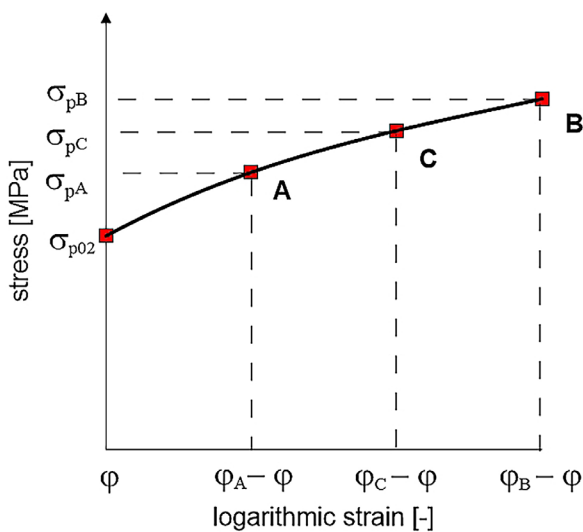$$\varphi_0 = \frac{\varphi_C^2 - \varphi_A \cdot \varphi_B}{\varphi_A + \varphi_B - 2\varphi_C} \tag{4}$$

$$n = \frac{\ln \sigma_B - \ln \sigma_A}{\ln(\varphi_0 + \varphi_B) - \ln(\varphi_0 + \varphi_A)} \tag{5}$$

while the constant C from the formula (6) for C_1 from the first equation from the system (2):

$$C_1 = \frac{\sigma_A}{(\varphi_0 + \varphi_B)^n} \tag{6}$$

The implementation of material models was carried out in the ABAQUS/CAE 2017 software, based on FEM. In this program, a computer simulation of the deep drawing process of cylindrical drawpieces from sheet blanks with a diameter of $D_0 = 66$ mm and a thickness of $s_0 = 1$ mm was carried out. The drawing coefficient $m_1 = 0.58$ was assumed. According to the literature [1], it was slightly higher than the limit drawing coefficient for the steel sheet (its theoretical minimum value is $m_t = 0.5$ for relative thickness of sheet $(s_0/D_0) \cdot 100 = 1.5$). Due to the shape of the cylindrical drawpiece, an axisymmetric problem was assumed in the calculations. The model consisted of two rigid elements, i.e. a punch and die, and a deformable blank for which an elastic-plastic material was assumed. The adopted model with boundary conditions is shown in the Figure 5.

The model assumes that the die is stationary and the punch performs a displacement of 35 mm. The sheet blank was filled with 50 elements of equal length, type SAX1 [20]. It is an axisymmetric linear shell element. The contact conditions between the tools and the elements of the deformed mesh were described by the friction coefficient $m = 0.1$.

Experimental verification of the deep drawing process was carried out on a stand consisting of the following elements (as shown in Figure 6):
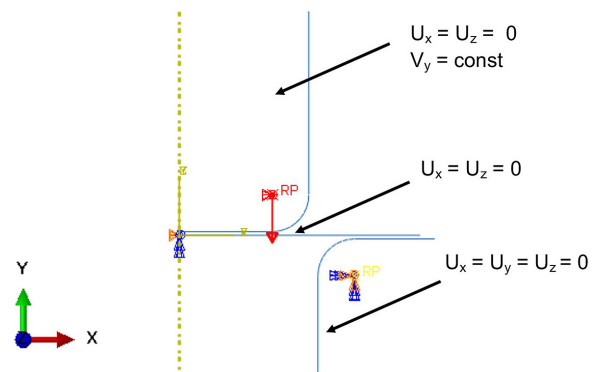

Fig. 4. The method of determining the points to determine the three-parameter equation of the strengthening curve

Fig. 5. The adopted model in computer modelling of deep drawing process with boundary conditions in ABAQUS software

Fig. 6. Experimental stand for deep drawing cylindrical drawpieces, where: 1 – ZD100 universal testing machine, 2 – Test&Motion software for measuring forces and displacements, 3 – laboratory press forming-die

- ZD100 universal testing machine, with a 1MN pressing force, modified by LABORTECH. It was calibrated and satisfies the metrological requirements for class 1;
- The laboratory press-tool [21] with the following dimensions: the punch diameter d_s = 35.5 mm, die diameter d_m = 38 mm, punch radius r_s = 5 mm and die radius r_m = 5 mm, respectively. Schematic representation of the tooling is shown in Figure 7;
- The computer test bench with specialized Test&Motion (LABORTECH) software for recording forces and displacements during tests.

A blank holder was used in the course of the deep drawing process (element 3 in Figure 7) because the literature-based condition of $s_0/D_0 \leq 0.02$ [1] was satisfied. The blank holder prevented the formation of folds and cracks in the material.

Both the simulation and experimental studies assumed a test speed of v = 80 mm/min.
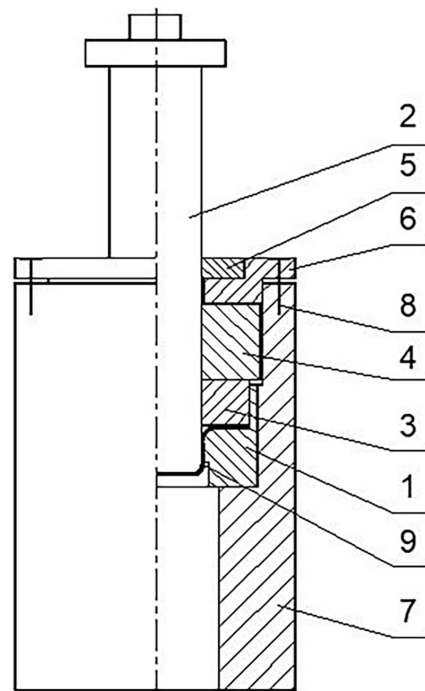

Fig. 7. Laboratory press-forming die for deep drawing of cylindrical drawpiece, where: 1 – die; 2 – punch; 3 – blank-holder; 4 – drawing ring; 5 – adjusting ring; 6 – cover of die holder; 7 – die holder; 8 – set screw; 9 – drawpiece

RESULTS AND ANALYSIS

Experimental investigations were carried out on the test pieces according to the methodology described in Chapter 2. Figure 3 shows the variation of tensile forces (F) as a function of displacement (Δl). Maximum force values were obtained for the following specimens: F = 6.177 kN at displacement Δl = 37.93 mm for brass, F = 5.424 kN at Δl = 25.49 mm for steel, F = 4.176 kN at Δl = 12.98 mm for copper and F = 2.184 kN at Δl = 2.16 mm for aluminium. These values are summarised in the last column of Table 1. The relative decreases in the recorded highest force values in relation to the maximum force for brass were respectively: 65% for aluminium, 60% for steel and 48% for copper. The smallest relative difference between the maximum forces occurred for the brass and steel samples (a decrease of 12%).

In the second stage of research, after determining the mechanical properties of aluminium, copper, brass and steel test pieces (as shown in Table 1), graphs of changes in flow stress versus relative strain were developed to refer the displacements to the length of the initial samples. They are presented in The flow stress σ_p was calculated from formula (7) [2, 3]:

$$\sigma_p = \frac{F}{S_0} \qquad (7)$$

where: F – force, N;
S_0 – initial test piece cross-section, mm².

The relative strain ε was calculated from the formula (8) [2, 3]:

$$\varepsilon = \frac{\Delta L}{L_0} \qquad (8)$$

where: ΔL – displacement, mm;
L_0 – initial length of the measuring part of the test piece, mm.

The highest stress values σ_p for the individual samples as R_m are shown in Table 2, for the aluminium sample at $\varepsilon = 0.029$, the copper sample at $\varepsilon = 0.173$, the brass sample at $\varepsilon = 0.506$ and the steel sample at $\varepsilon = 0.340$, respectively (as shown in Figure 8). The greatest difference between the maximum stresses σ_p occurred between the brass and aluminium samples (a decrease of approximately 68%). In contrast, the smallest difference was observed between the brass and steel samples (14% decrease).

It is noteworthy that in Figure 8, the highest relative strain ε was obtained for steel and brass specimens. It was similar and amounted to $\varepsilon = 0.52$. For the drawing of flangeless cylindrical drawpieces from steel sheets, the literature [1] states that the minimum drawing factors for the first operation (first draw) are, on average, about 0.5 (exactly 0.45 to 0.63 depending on the relative thickness s_0/D_0, where s_0 is the thickness of the material and D_0 the diameter of the blank), in order to prevent cracking of the material. This means that for the first operation (first draw), the maximum total deformation ε_c is also about 0.5 (because $\varepsilon_c = 1 - m_l$, where m_l is the minimum deformation factor for the first draw [1]). This value makes it possible to shape a flangeless cylindrical drawpiece without intermediate annealing. According to the author's opinion, it is possible to relate the value of the maximum relative elongation ε obtained in Figure 8 for steel to the total elongation ε_c from the literature [1] in a somewhat simplified manner. This is evidenced by the fact that for values above 0.5, material fracture (both of the tensile specimen and the cylindrical drawpiece) occurs with high probability in both cases.

Figure 9 shows experimental strengthening curves. The strain in the graphs was calculated as axial logarithmic strain φ from formula (9) [2,3]:
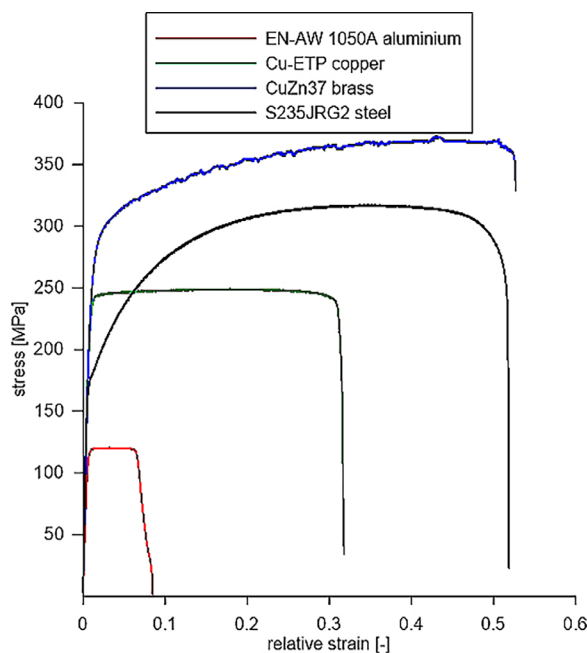

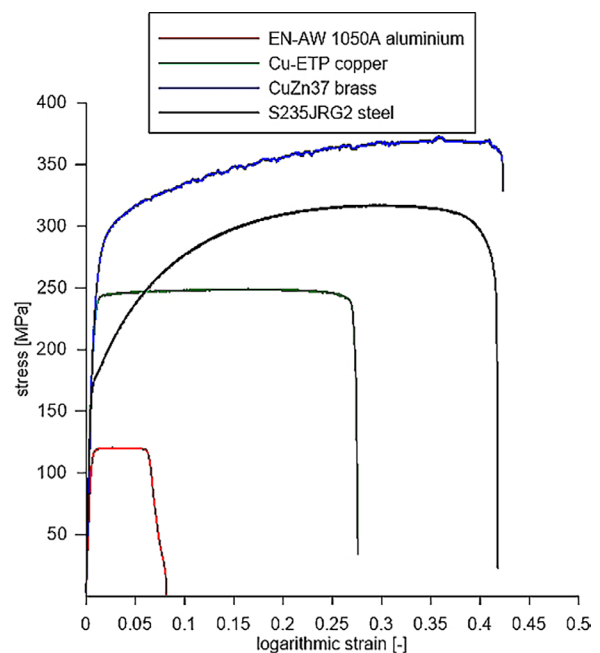**Fig. 8.** The flow stress (σ_p) vs. relative strain (e) obtained for tensile tests

Fig. 9. Strengthening curves obtained experimentally (the flow stress σ_p vs. axial logarithmic strain φ)

$$\varphi = \ln \frac{L}{L_0} \qquad (9)$$

where: L − the current length of the measuring part of the test piece, mm.

In Figure 9, two groups of similarly behaving materials can be observed. The samples with higher strength properties, i.e. steel and brass, showed strengthening curve characteristics corresponding to materials that were in the as-annealed condition. They have the ability to strengthen in the initial phase of plastic deformation. The second group consists of specimens made of materials with lower strength properties, i.e. copper and aluminium alloy. According to the characteristics of the strengthening curves, it is likely that they were given an initial deformation, as evidenced by the relatively high flow stress value for small deformations and the flat course of the graph.

In the next stage of the research, the experimental strengthening curves were approximated with the three-parameter function (1). Points A, B and C for the system of equations (2) were selected between the yield strength point and the tensile strength of the test pieces according to literature recommendations [2] for materials that are in the as-unknown condition. Graphical representation of the proposed solution on the actual strengthening curve for the tested materials is shown in Figure 10. Points A were selected near the yield point (slightly above by about 1%), points B had values close to tensile strength values, and points C had values of yield stress approximately as the arithmetic mean between stress values at points A and B.

The calculated values of coefficients C, φ_0 and n are presented in Table 3. On their basis, equations describing strengthening curves are given in Table 4. In all cases for the materials tested, the strain φ_0
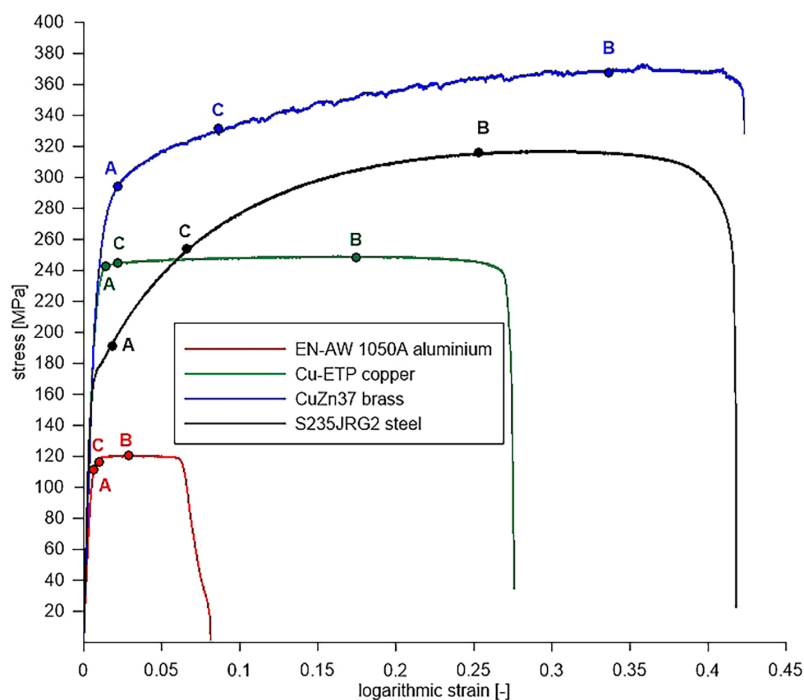

Fig. 10. Arrangement of points A, B and C on the actual strengthening curve for the tested materials

Table 3. Values of calculated parameters for three-parameter functions describing strengthening curves

Material	C (MPa)	φ_0 (MPa)	n (-)
EN-AW 1050A aluminium	125	-0.00109	0.012
Cu-ETP copper	252	0.000435	0.0066
CuZn37 brass	403	-0.01959	0.08
S235JRG2 steel	395	0.00985	0.16

Table 4. Equations describing strengthening curves

Material	equations with calculated coefficients	equations after rounding of the coefficients
EN-AW 1050A aluminium	$\sigma_p = 125 \cdot (-0.00109 + \varphi)^{0.012}$	$\sigma_p = 125 \cdot \varphi^{0.012}$
Cu-ETP copper	$\sigma_p = 252 \cdot (0.000435 + \varphi)^{0.0066}$	$\sigma_p = 252 \cdot \varphi^{0.01}$
CuZn37 brass	$\sigma_p = 403 \cdot (-0.01959 + \varphi)^{0.08}$	$\sigma_p = 403 \cdot \varphi^{0.1}$
S235JRG2 steel	$\sigma_p = 395 \cdot (0.00985 + \varphi)^{0.16}$	$\sigma_p = 395 \cdot (0.01 + \varphi)^{0.2}$

takes values close to zero. Therefore, it can be assumed without fear of error that the three-parameter expression of the strengthening curve simplifies to a two-parameter form as for annealed materials (as shown in the second column of Table 4).

From the analysis of the experimental strengthening curves (shown in Figure 9), this confirms the earlier conclusion for brass and steel. What is puzzling, however, is the fact of the near-zero φ_0 deformations for copper and aluminium, which in the experimental curves show a pre-strengthened state. It is likely that such values calculated from equation (4) were determined by the too small distances between points A, B, C lying between the yield strength and tensile strength (and the corresponding very small changes in strains φ_A, φ_B and φ_C, respectively), since the differences between R_m and $R_{p0.2}$ were only about 7% for aluminium and 4% for copper (second and third columns in Table 2).

On the basis of the determined coefficients and equations, the graph shown in Figures 11 was prepared for tested materials.
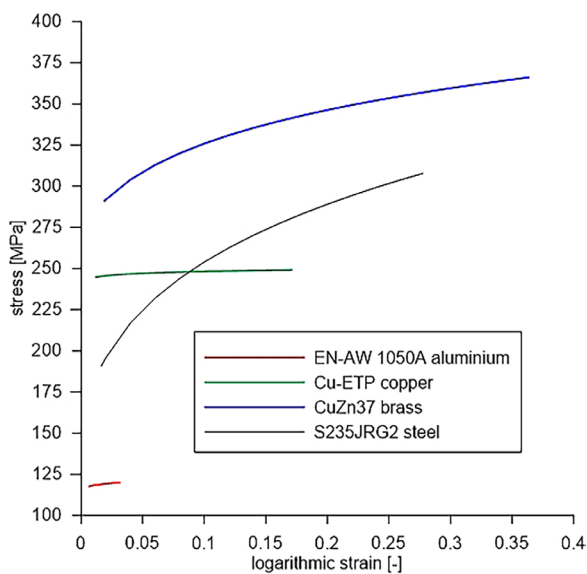

Fig. 11. Strengthening curves calculated with a three-parameter function for tested materials

It is noted that the presented analytically determined strengthening curves represent only the sections between yield strength and tensile strength. For materials after initial strain hardening such as aluminium and copper, the flow stress σ_p values on graph are very close to the material constant C values against very low exponents n. Sections of the strengthening curves for brass and steel are similar in nature. They follow a course resembling to the changes characteristic of annealed materials. The equations have very similar analytically determined material constants C and different strengthening exponents n ($C = 403$ MPa, $n = 0.1$ for brass and $C = 395$ MPa, $n = 0.2$ for steel) as shown in Table 4 after rounding off the values. For logarithmic (equivalent) strains φ smaller than $\varphi = 0.36$ for brass and $\varphi = 0.29$ for steel respectively, due to the lower value of the exponent n, the flow stress values σ_p for brass increase much faster than for steel. Pre-strain coefficients φ_0 close to zero for both specimens may confirm the lack of previously imparted strengthening.

In order to validate them, the developed material models were used in a computer simulation of the deep drawing process of cylindrical drawpieces from metal sheets. Using an steel drawpiece as an example, the successive stages of material formation in a modelling are shown in the Figure 12.

The numerical force waveforms in the punch displacement function for deep drawing process were obtained, which are presented in the Figure 13. They are very similar in nature, regardless of the kind of tested materials at the same degree of drawpieces deformation (relative deformation is $e = 1 - m_1 = 1 - 0.58 = 0.42$). In the course of deep drawing, pressing forces changed depending on the punch displacement (or drawpiece height). The punch path at which the drawing forces obtain maximum value relative to the total path in the course of drawing was 0.3, 0.45 for the single drawing operation. The highest value of the maximum numerical force was obtained for brass, and
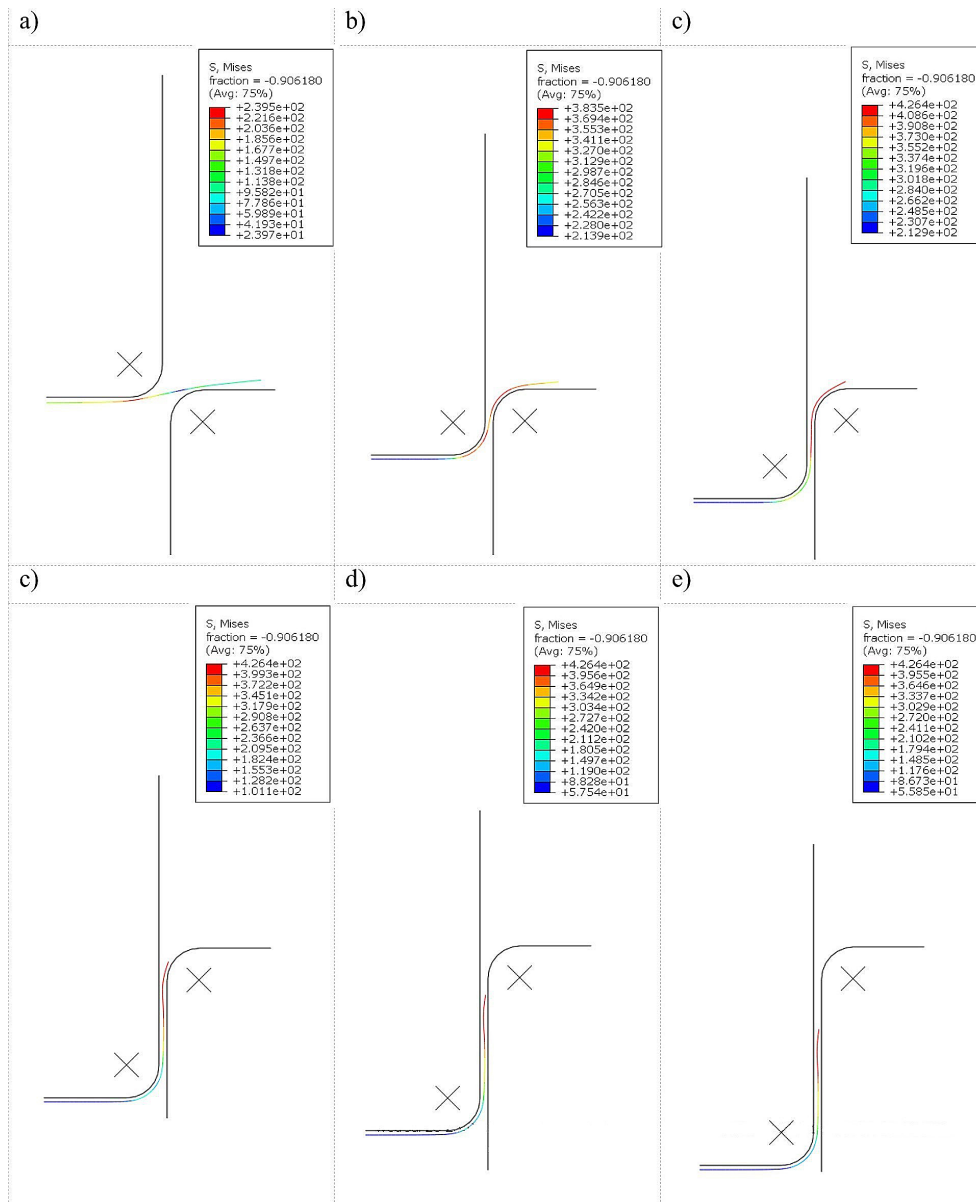
Fig. 12. Numerically calculated stages a–f. of deep drawing of cylindrical drawpiece from S235JRG2 steel

the lowest for aluminium (30.939 kN and 9.533 kN respectively).

As part of the experimental verification of the modelling results obtained with regard to the variation of forces as a function of displacement, the deep drawing process of cylindrical drawpieces was carried out under laboratory conditions with the assumptions and on the stand described before. The result of the experimental tests of the deep drawing process were the drawpieces shown in Figure 14. The outer diameters of the resulting drawpieces made from each material were similar to each other (they were approximately 37.8 mm). The average wall thicknesses measured at mid-height of the specimens were close to the initial thicknesses of the sheet blanks given in Table 1

as a_0 and showed a slight thickening relative to the initial material. The increase in thickness in this zone did not exceed 2% for aluminium and steel and 5% for copper and 6% for brass, respectively. The highest average drawpiece height was obtained for steel, at 23.1 mm. For the other samples, the average heights were comparable and were 22.8 mm for aluminium, 22.7 mm for copper and 22.6 mm for brass, respectively. There were no defects in the resulting drawpieces shown in Figure 14 in the form of material folding or cracking.

Experimental force waveforms were recorded during their shaping, as shown in Figure 15. The nature of these force changes for individual materials is similar to numerical graphs (as shown
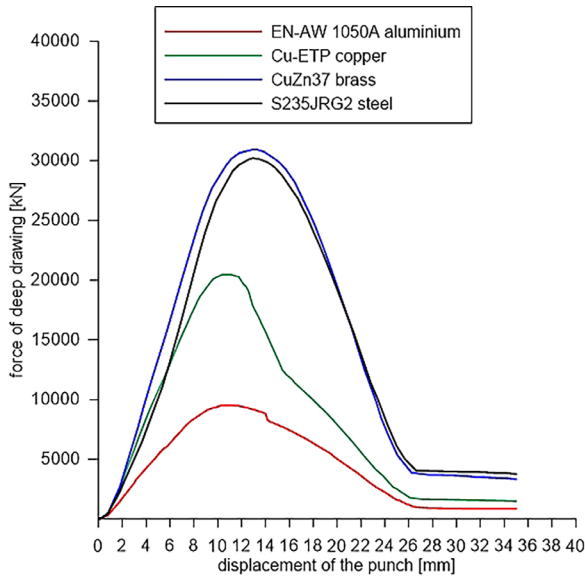
Fig. 13. Numerically obtained changes of deep drawing forces vs. displacement for the tested materials
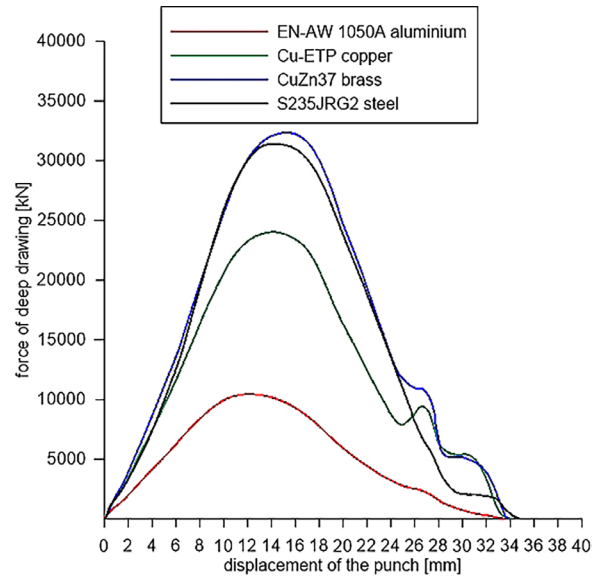

Fig. 15. Experimentally obtained changes of deep drawing forces vs. displacement for the tested materials

in Figure 13). Also as in modelling, the highest maximum force was obtained for brass and the smallest for aluminium (32.338 kN and 10.453 kN respectively).

Based on the graphs in Figure 13 and Figure 15, the maximum values of the forces in the computer simulation and experimental tests of the deep drawing process of cylindrical drawpieces from the tested materials are summarised in Table 5.

In each case, the maximum force values obtained in the experiment were greater than those

from modelling. The relative decrease of the values of numerical forces in relation to the experimental forces for the tested materials was as follows: for aluminium 8.79%, for copper 14.85%, for brass 4.33% and steel 4.05%. In the author's opinion, such differences not exceeding 15% are acceptable in engineering practice and testify to the correct implementation of the developed material models in ABAQUS software. In similar studies of the deep drawing process from aluminium sheets, Różyło and Wójcik [22] obtained relative

Fig. 14. Experimentally obtained drawpieces from the tested materials

Table 5. Summary of maximum numerical F_N and experimental F_D values of deep drawing forces

Material	F_N (kN)	F_D (kN)
EN-AW 1050A aluminium	9.533	10.453
Cu-ETP copper	20.462	24.031
CuZn37 brass	3.939	32.338
S235JRG2 steel	30.119	31.389

differences between the maximum numerical and experimental forces from 5.1% to 16%, depending on the software applied (ABAQUS and DE-FORM, respectively). In their research, they used, among other things, a blank with a diameter of 50 mm and a thickness of 1 mm. For the punch and die dimensions they applied, the drawing ratio can be estimated and found to be very similar (around 0.60 versus 0.58 in the paper). A direct comparison of the differences obtained by the authors [22] and in this paper is not possible, as Różyło and Wójcik did not specify the friction coefficient, which they adopted in modelling, and which has a very significant effect on the numerical change of force as a function of displacement in the deep drawing process. In addition, in their research they used different radii for the rounding of the punch and die which also has an impact on the change and values of the stamping force. Their research [22] confirmed the existence of similar differences to those in the paper between the experimental and numerical maximum pressing forces.

CONCLUSIONS

Based on the study of the determination of strengthening curves by experimental and analytical methods for EN-AW 1050A aluminium, Cu-ETP copper, CuZn37 brass and S235JRG2 steel, it was found:
1. The test pieces made of steel and brass have the characteristics of recrystallised annealed material, while the analysis of the strengthening curves of the samples made of copper and aluminium sheet suggests a material in the as-rolled condition.
2. The method of approximating the experimental strengthening curve with a three-parameter equation may be ineffective for determining the initial strain φ_0 especially for pre-strengthened materials having very small differences between yield and tensile strength (such as about 7% for aluminium and 4% for copper) and with a flattened shape of the graphs. Such a case does not allow a suitable choice of three points for approximation with significant differences in deformation allowing φ_0 to be calculated.
3. From the point of view of preparing boundary material data for the simulation of sheet metal forming processes, in the form of a hardening curve, it is most advantageous to enter it into an FEM-based programme as a text file with experimental data of flow stresses and logarithmic (equivalent) strains. Introducing a ready-made equation of the strengthening curve into the program, especially for pre-strengthened materials, is an option that always includes some simplification.
4. The results obtained in the research can be used in industrial practice for computer-aided design of cold-deep drawing processes for components of simply shapes. It was demonstrated by implementing the developed material models for computer simulation of the deep drawing process of cylindrical drawpieces. The differences found between the maximum numerical and experimental values of the pressing forces did not exceed about 15% for copper, 10% for aluminium and 5% for brass and steel.

REFERENCES

1. Pacanowski J. *Design of deep drawing process of axisymmetric drawpieces and design press-forming dies T1 Methods and directives for deep drawing of axisymmetric drawpieces* (Kielce: Kielce University of Technology), 2018, 471(in Polish).
2. Marciniak Z. *Limit strains in deep drawing process of sheet metals* (Warsaw: WNT) chapter 7, 1971, 189-225 (in Polish).
3. Lange K. Handbook of metal forming. McGraw--Hill Book Company, 1985.
4. Gronostajski Z., Pater Z., Madej L., Gontarz A., Lisiecki L., Łukaszek-Sołek A., Łuksza J., Mróz S., Muskalski Z., Muzykiewicz W., Pietrzyk M., Śliwa R.E. Tomczak, J. Wiewiórowska S., Winiarski G., Zasadziński J., Ziółkiewicz S. Recent development trends in metal forming. Archives of Civil and Mechanical Engineering 2019; 19(3): 898–941.
5. Rousselier G., Barlat F., Yoon J.W. A novel approach for modelling of anisotropic hardening and non proportional loading paths, application to finite element analysis of deep drawing. International Journal of Material Forming 2009; 2: 367–370.
6. Merklein M., Gödel V. Characterization of the flow behaviour of deep drawing steel grades in dependency of the stress state and its impact on fea. International Journal of Material Forming 2009; 2: 415-41.
7. Bressan J.D., Divo J., Cieto J., C., Vieira F., H., Bastos L.S.B., Rojas P.A.M.A Numerical simulation study of deep drawing testing and experimental results of steel sheets, using a comercial software. International Journal of Material Forming 2010; 3: 231–234.
8. Trzepieciński T., Gelgele H.L. Investigation of anisotropy problems in sheet metal forming using finite element method. International Journal of Material Forming 2011; 4: 357–369.

9. Peters P., Manopulo N., Lange Ch., Hora P. A strain rate dependent anisotropic hardening model and its validation through deep drawing experiments. International Journal of Material Forming 2014; 7: 447–457.

10. Dizaji S.A., Darendeliler H., Kaftanoğlu B. Effect of hardening models on different ductile fracture criteria in sheet metal forming. International Journal of Material Forming 2016; 9: 261–267.

11. El-Aty A.A., Xu Y., Guo X., Zhang S-H., Ma Y., Chen D. Strengthening mechanisms, deformation behavior, and anisotropic mechanical properties of Al-Li alloys: A review. Journal of Advanced Research 2018; 10: 49–67.

12. Ruiz-Pinilla J.G., Montoya-Coronado L.A., Cladera A. Finite element modelling of RC beams externally strengthened with iron-based shape memory alloy (Fe-SMA) strips, including analytical stress-strain curves for Fe-SMA. Engineering Structures 2020; 223: 1–12.

13. Feng Z., Yoon S-Y., Choi J-H., Barrett T.J., Zecevic M., Barlat F., Knezevic M. A comparative study between elasto-plastic self-consistent crystal plasticity and anisotropic yield function with distortional hardening formulations for sheet metal forming. Mechanics of Materials 2020; 148: 1–13.

14. Walzer S., Liewald M. Novel approach to decrease sheet thinning during sheet metal forming by using embossing technique. Procedia Manufacturing 2020; 50: 795–799.

15. Habraken A.M. et al. Analysis of ESAFORM 2021 cup drawing benchmark of an Al alloy, critical factors for accuracy and efficiency of FE simulations. International Journal of Material Forming 2022; 15 (61): 1–96.

16. Szala M., Winiarski G., Wójcik Ł., Bulzak T. Effect of annealing time and temperature parameters on the microstructure, hardness, and strain-hardening coefficients of 42CrMo4 steel. Materials 2020; 13(9):1–16.

17. Winiarski G., Samołyk G. New methodology for predicting the cracking phenomenon in the radial extrusion process of hollow parts with a flange. Advances in Science and Technology Research Journal 2023; 17(3): 64–72.

18. Miłek T., Kowalik B., Kuliński B. Evaluation of the possibility of performing cold backward extrusion of axisymmetric thin-walled aluminium die stampings with square section. Archives of Metallurgy and Materials 2015; 60(4): 3043–3049.

19. ISO, E., 6892-1. Metallic materials - Tensile testing - Part 1: Method of test at room temperature, International Organization for Standardization, 2019.

20. Hughes T.J.R., Taylor R.L., Kanoknukulchai W. A simple and efficient element for plate bending. International Journal for Numerical Methods in Engineering 1977; 11(10): 1529–1543.

21. Miłek T. Evaluation of the possibility of deep drawing of aluminium cylindrical drawpieces from sheets at different relative rolling reductions. Journal of Physics. Conference Series 2021; 1736: 1–8.

22. Różyło P., Wójcik Ł. FEM and experimental based analysis of the stamping process of aluminum alloy. Advances in Science and Technology Research Journal 2017; 11(3): 94–101.